

# Journal of Materials Science: Materials in Electronics

## Vibrational Spectroscopic Studies on Crystallisation of Sol-Gel Derived Thin Films of Calcia-Alumina Binary Compound

--Manuscript Draft--

<b>Manuscript Number:</b>	JMSE-D-14-00099
<b>Full Title:</b>	Vibrational Spectroscopic Studies on Crystallisation of Sol-Gel Derived Thin Films of Calcia-Alumina Binary Compound
<b>Article Type:</b>	Original Research
<b>Keywords:</b>	Sol-gel, Raman Spectroscopy, Phase transformations, single phase calcia-alumina binary films
<b>Corresponding Author:</b>	Asim K Ray Brunel University Middlesex, UNITED KINGDOM
<b>Corresponding Author Secondary Information:</b>	
<b>Corresponding Author's Institution:</b>	Brunel University
<b>Corresponding Author's Secondary Institution:</b>	
<b>First Author:</b>	Elnaz Feizi
<b>First Author Secondary Information:</b>	
<b>Order of Authors:</b>	Elnaz Feizi Jesus J. Ojeda Asim K Ray
<b>Order of Authors Secondary Information:</b>	
<b>Abstract:</b>	An optimized sol-gel process has now been developed to produce homogeneous thin films of calcium aluminate binary $12\text{CaO} \cdot 7\text{Al}_2\text{O}_3$ compound, $12\text{CaO} \cdot 7\text{Al}_2\text{O}_3$ , on magnesium oxide substrates via spin coating. Fourier transform infrared (FTIR) and Raman spectroscopies have been employed to investigate the effect of annealing temperature and duration on the phase transformations in the films. Heat treatment at $13000\text{C}$ under air atmosphere for 2 hours produced single-phase $12\text{CaO} \cdot 7\text{Al}_2\text{O}_3$ films. However, annealing at a lower temperature of $11000\text{C}$ in air for a period of 4 hours in total resulted in the crystallization of $5\text{CaO} \cdot 3\text{Al}_2\text{O}_3$ rather than $12\text{CaO} \cdot 7\text{Al}_2\text{O}_3$ . The X-ray photoelectron spectrum of the thin film annealed at $13000\text{C}$ corresponds to the binding energies of C12A7 compound. The annealing temperature of $13000\text{C}$ for 2 hours is found to be sufficient for formulating single phase calcia-alumina binary films in correct stoichiometric ratio of 12:7.

1  
2  
3  
4 **Vibrational Spectroscopic Studies on Crystallisation of Sol-Gel Derived**  
5  
6 **Thin Films of Calcia-Alumina Binary Compound**  
7

8  
9 Elnaz Feizi<sup>1</sup>, Jesus J. Ojeda<sup>2</sup> and Asim K. Ray<sup>1\*</sup>

10  
11  
12 <sup>1</sup>Centre for Materials Research, Queen Mary, University of London, Mile End Road, London  
13 E1 4NS, UK

14  
15 <sup>2</sup> Experimental Techniques Centre, Brunel University, Uxbridge, Middlesex UB8 3PH, UK  
16

17  
18 **Abstract**

19 An optimized sol-gel process has now been developed to produce homogeneous thin films of calcium  
20 aluminate binary  $12\text{CaO}\cdot 7\text{Al}_2\text{O}_3$  compound,  $12\text{CaO}\cdot 7\text{Al}_2\text{O}_3$ , on magnesium oxide substrates via spin  
21 coating. Fourier transform infrared (FTIR) and Raman spectroscopies have been employed to  
22 investigate the effect of annealing temperature and duration on the phase transformations in the films.  
23 Heat treatment at  $1300^\circ\text{C}$  under air atmosphere for 2 hours produced single-phase  $12\text{CaO}\cdot 7\text{Al}_2\text{O}_3$   
24 films. However, annealing at a lower temperature of  $1100^\circ\text{C}$  in air for a period of 4 hours in total  
25 resulted in the crystallization of  $5\text{CaO}\cdot 3\text{Al}_2\text{O}_3$  rather than  $12\text{CaO}\cdot 7\text{Al}_2\text{O}_3$ . The X-ray photoelectron  
26 spectrum of the thin film annealed at  $1300^\circ\text{C}$  corresponds to the binding energies of C12A7  
27 compound. The annealing temperature of  $1300^\circ\text{C}$  for 2 hours is found to be sufficient for formulating  
28 single phase calcia-alumina binary films in correct stoichiometric ratio of 12:7.  
29  
30  
31  
32  
33  
34  
35  
36  
37  
38  
39  
40  
41  
42  
43  
44  
45  
46  
47  
48  
49  
50  
51  
52  
53  
54  
55  
56

57  
58 

---

  
59 \* Present address: The Wolfson Centre for Materials Processing, Brunel University, Uxbridge,  
60 Middlesex UB8 3PH, UK  
61  
62  
63  
64  
65

## 1. INTRODUCTION

Recent developments in the field of thin-film-based optoelectronic devices, such as thin film transparent transistors and solar cells, have led to an increasing interest in the fabrication of high quality thin films of insulating, semiconducting and conducting types in order to achieve a high efficiency and improved chemical stability in different environments. The calcia-alumina binary compound  $12\text{CaO}\cdot 7\text{Al}_2\text{O}_3$ , or C12A7, has been widely known for several years as one of the main constituents of calcium aluminate cements. However, it has been recently discovered that it can be used as a fast oxide-ion conductor due to its unique structure [1]. The stoichiometric chemical composition of the unit cell is represented as  $[\text{Ca}_{24}\text{Al}_{28}\text{O}_{64}]^{4+}\cdot 2\text{O}^{2-}$  in which  $[\text{Ca}_{24}\text{Al}_{28}\text{O}_{64}]^{4+}$  is the positively charged framework with 12 sub-nanometer-sized cages [2-4]. This means that each cage has a mean charge of +1/3. In order to compensate for the positive charge of the framework, two  $\text{O}^{2-}$  oxygen ions are incorporated in each unit cell and distributed randomly inside 2 out of 12 cages. The incorporated oxygen ions in C12A7 structure can be replaced by other anions, such as  $\text{O}^-$ ,  $\text{O}_2^{2-}$ ,  $\text{OH}^-$ , or even by electrons and the material exhibits different physical properties depending on the type of incorporated anions without a significant change in the structure of the lattice. C12A7 has gained much attention for potential applications in various fields, such as ion conducting solid electrolyte, reducing agent, cold-cathode electron field emitter, oxidizing catalyst, ion emitter and as a transparent conductive oxide in flat panel displays, solar cells and transparent transistors [5, 6].

While the fabrication of C12A7 single crystal and polycrystalline bulk has been studied extensively during the last few years, studies on the fabrication of C12A7 thin films are rather limited. The thin film fabrication techniques include pulsed laser deposition and sol-gel method, and magnesium oxide (MgO) single crystal is used as the substrate. A heat treatment temperature of 1100 °C in air atmosphere has been suggested for the crystallization of amorphous thin films prepared via pulsed laser deposition [7, 8], while this temperature is mentioned to be too low for the crystallization of the sol-gel derived films [9].

The fabrication of C12A7 thin films via sol-gel technique has been previously reported employing ethyl acetoacetate (EAA) and aluminium sec-butoxide (ASB) as a chelating agent and the main precursor of aluminium oxide, respectively in the molar ratio of 1:1 in an ethanol solvent. Hydrochloric acid (HCl) was used as the pH regulator [10, 11]. However, our initial attempt in the deposition of C12A7 thin films on the MgO substrates using this recipe resulted in the formation of discontinuous films with dendritic growth behaviour. Therefore, the solution recipe was modified in

1  
2  
3  
4 order to increase the homogeneity and continuity of the films. Highly stable spreading solutions for  
5 spin coating were obtained using the modified recipe without the need for the addition of acid. This  
6 article presents the Fourier transform infrared (FTIR) and Raman spectroscopy investigations into  
7 the effect of heat treatment temperature and duration on the formation of sol-gel derived C12A7 thin  
8 films on magnesium oxide substrates. The compositional analysis of the sol-gel derived films is  
9 quite challenging due to the low thickness of the films and the interference from the substrate. ATR-  
10 FTIR spectroscopy (Attenuated Total Reflectance) and Raman spectroscopy have been successfully  
11 employed in order to identify different calcium aluminate phases which are formed at different heat  
12 treatment temperatures and durations. The formation of C12A7 phase is further confirmed by X-ray  
13 photoelectron spectroscopy. An appropriate heat treatment procedure is, therefore, suggested for the  
14 fabrication of sol-gel derived C12A7 thin films based on the FTIR and Raman spectral analyses.

## 23 **2. EXPERIMENTAL DETAILS**

24  
25 For the sol-gel formulation, the solution was prepared using stoichiometric ratios of aluminium  
26 sec-butoxide (ASB) and calcium nitrate tetrahydrate ( $\text{H}_8\text{CaN}_2\text{O}_{10}$ ) as the main precursors of  
27 aluminium oxide and calcium oxide respectively. The solutions containing each precursor were  
28 prepared separately and then mixed during the last step of the preparation. Since aluminium sec-  
29 butoxide is highly sensitive to the presence of water, ethyl acetoacetate (EAA) was chosen as a  
30 chelating agent. The EAA-to-ASB molar ratio was increased to 2:1 and isopropyl alcohol was used  
31 as the solvent with a molar ratio of 10:1 for both solvent-to-ASB and solvent-to-calcium nitrate  
32 ratios. Deionized water was mixed with the nitrate solution and then added to the alkoxide solution  
33 with water-to-ASB molar ratio of 5:1, forming highly stable spreading solutions for spin coating. A  
34 KW-4A spin coater was used for or 30s at the speed of 1000rpm to deposit 5 – 6 $\mu\text{m}$  thick films on  
35 ultrasonically cleaned on 10 mm $\times$ 10 mm $\times$ 0.5mm magnesium oxide (MgO) single crystal substrates.  
36 All the samples were left drying slowly for at least 2 days prior to the heat treatment. The dried films  
37 were isothermally annealed at 1100 $^\circ\text{C}$  and 1300 $^\circ\text{C}$  for the duration between 2hr and 5 hr under air  
38 atmosphere for the phase and compositional analysis via Attenuated Total Reflectance-Fourier  
39 Transform Infrared (ATR-FTIR), Raman and X-ray photoelectron (XPS) spectroscopies. The effect  
40 of heat treatment on the surface morphology of the films was examined with the help of a JEOL  
41 JSM-6300 field-emission scanning electron microscope in a magnification range of 50 – 50000X

42  
43  
44  
45  
46  
47  
48  
49  
50  
51  
52  
53  
54  
55  
56 Using a Spectrum 100 FTIR instrument equipped with diamond ATR accessory (Perkin Elmer),  
57 the infrared spectra for differently heated samples were obtained in a range of 400 – 4000  $\text{cm}^{-1}$  with  
58 a resolution of 4  $\text{cm}^{-1}$  and accumulation of 100 scans per test. A sample area of 3 mm $\times$ 3 mm was in  
59  
60  
61  
62  
63  
64  
65

1  
2  
3  
4 contact with the diamond for each measurement and the data was collected from at least 5 randomly  
5 selected areas of the surface in order to ensure the reproducibility of the results. A Nicolet Almega  
6 XR Raman spectrometer (Thermo Scientific) was employed to record the Raman spectra in a range  
7 of 40–4200  $\text{cm}^{-1}$  for wave numbers using the laser beam wavelengths of 532 and 785 nm.  
8  
9

10  
11 The elemental composition analysis was performed using a VG ESCALAB 210 X-ray  
12 photoelectron spectrometer (XPS) fitted with a non-monochromatic Al  $K\alpha$  X-ray source (1486.6 eV)  
13 capable of operating with an X-ray emission current of 20 mA and an acceleration voltage of 12 kV.  
14 The take-off angle was fixed at  $90^\circ$  with the nominal analysis depth of 10 nm. The area  
15 corresponding to each acquisition was a rectangle of  $5\text{ mm} \times 2\text{ mm}$ . Each analysis consisted of wide  
16 survey scans (pass energy 50 eV, 1.0 eV step size) and high-resolution scans (pass energy  
17 50 eV, 0.05 eV step size) for component speciation. The numbers of scans were 10 and 5 for the  
18 survey spectra and each expansion respectively. The binding energy scale was calibrated using the  
19 Au  $4f_{5/2}$  (83.9 eV), Cu  $2p_{3/2}$  (932.7 eV) and Ag  $3d_{5/2}$  (368.27 eV) lines of cleaned gold, copper and  
20 silver standards from the National Physical Laboratory (NPL), UK. The charge effects were  
21 corrected using the position of the C1s peak at 284.5 eV.  
22  
23  
24  
25  
26  
27  
28  
29  
30

### 31 **3. RESULTS AND DISCUSSION**

32  
33 The microstructure of the thin film in Figure 1 shows that the surface continuity of the film was  
34 preserved even after the heat treatment at  $1300^\circ\text{C}$  for 2 hr in air atmosphere and no cracks or scales  
35 were observed. A completely crystallized structure was formed with well-defined grain boundaries  
36 but with no trace of dendrite structure.  
37  
38  
39  
40

41  
42 Two calcium aluminate thin films on MgO substrates were individually annealed at  $1100^\circ\text{C}$  for 4hr  
43 and  $1300^\circ\text{C}$  for 2hr. The absorption peaks in the IR spectrum in Figure 2(a) show that a thin film  
44 which was annealed at  $1100^\circ\text{C}$  for 4 hr is pentacalcium trialuminate  $5\text{CaO} \cdot 3\text{Al}_2\text{O}_3$  (C5A3) but not  
45 C12A7. This formation may be attributed to a restrained crystallization of C12A7 on MgO substrate.  
46 C12A7 and C5A3 are quite similar in chemical composition with 48.5 and 47.8 % mass of CaO  
47 respectively [12]. However, they are not considered as polymorphs and are believed to form under  
48 different heat treatment atmospheres [13]. The main difference between these two phases is the  
49 absence of a nanoporous structure in C5A3 [14]. The  $\text{AlO}_4$  tetrahedra in C5A3 form a network of  
50 five rings with a layered arrangement of Ca atoms. In C12A7, however, three irregular Ca octahedra  
51 share an edge and are joined with an Al tetrahedron through a four-coordinated oxygen atom  
52 forming a two-dimensional sheet structure.  
53  
54  
55  
56  
57  
58  
59  
60  
61  
62  
63  
64  
65

1  
2  
3  
4 In order to investigate the possibility of a phase transformation from C5A3 to C12A7, C5A3 thin  
5 films were additionally heat treated at 1300°C for 2hr. The heat treatment duration was kept at 2 hr  
6 in order to minimize any possible chemical reactions at the film-substrate interface and ensure the  
7 crystallization of the film. The FTIR spectrum of a thin film heat treated at 1300 °C for a further  
8 duration of 2hr is depicted in Figure 2(b). The phase analysis of the film shows a progress towards  
9 the formation of C12A7. Two new peaks appearing at 465 and 848 cm<sup>-1</sup> are in good match with the  
10 IR peaks observed for C12A7 [15]. It has been reported that C5A3 transforms into C12A7 in the  
11 presence of oxygen in the atmosphere. The appearance of the two high-intensity absorption peaks at  
12 465 and 848 cm<sup>-1</sup> and the non-existence of all C5A3 medium-to-high intensity peaks confirm that  
13 the temperature of 1300 °C is high enough for the preferable formation of C12A7 for the duration of  
14 2 hr. The related symmetry and origin of these bands are given in Table 1. Although some of the  
15 absorption peaks of C12A7 and C5A3 might be positioned at similar frequencies, the sharp  
16 absorption peak at 848 cm<sup>-1</sup> is characteristic of C12A7. This absorption peak is the fundamental  
17 absorption band of C12A7 and corresponds to the vibration modes of the bonded tetrahedra Al-O  
18 bonds. A summary of the observed FTIR absorption bands of the C12A7 thin films along with the  
19 possible vibrational modes and the origin of these vibrations are given in Table 1.  
20  
21  
22  
23  
24  
25  
26  
27  
28  
29  
30  
31

32 The Raman spectrum of a thin film heat treated at 1100 °C for 4 hr is shown in Figure 3(a). The  
33 result of the Raman spectral analysis shows the formation of C5A3 after a heat treatment at 1100 °C  
34 which is in accordance with FTIR results in Figure 2(a). Although some of the Raman-sensitive  
35 peak positions of C5A3 are rather similar to C12A7, the appearance of a high-intensity peak at  
36 ~ 600 cm<sup>-1</sup> is characteristic of C5A3 phase. A few additional bands are also observed in the  
37 spectrum of C5A3, such as 348, 440 and 753 cm<sup>-1</sup>, which can be useful in order to distinguish  
38 between the two phases. The Raman spectrum of a thin film after a heat treatment at 1300 °C for 2  
39 hr is depicted in Figure 3(b). The result of the Raman spectroscopy of the film is in accordance with  
40 the FTIR analysis. Both spectra confirm the formation of C12A7 after a heat treatment at 1300 °C  
41 under air atmosphere. The high-intensity band at 517 cm<sup>-1</sup> and medium-intensity band at  
42 779 cm<sup>-1</sup> are exclusively characteristic of C12A7 phase.  
43  
44  
45  
46  
47  
48  
49  
50  
51  
52  
53  
54

55 The symmetries determined for each vibrational frequency (Table 2) can be represented via the  
56 following relation suggested for the total number of vibrational modes for C12A7 framework:  
57  
58  
59  
60  
61  
62  
63  
64  
65

1  
2  
3  
4  $\Gamma_v^{opt} = 6A_1(Raman) + 7A_2 + 13E(Raman) + 22F_1 + 22F_2(IR, Raman)$   
5  
6  
7

8 Among these vibration modes,  $A_1$ ,  $E$  and  $F_2$  are Raman active and only  $F_2$  is IR active. Since the  
9 number of Raman-sensitive vibrational modes in C12A7 framework is higher than the FTIR-  
10 sensitive modes, more information can be obtained from the Raman spectrum of this compound  
11 compared to FTIR spectrum.  
12  
13  
14

15 It is to be noted that due to the limitations of the ATR-FTIR equipment, the IR spectrum was only  
16 obtained down to a wavenumber of  $400\text{ cm}^{-1}$  and therefore, it was not possible to compare the peaks  
17 of Raman spectroscopy to the ones of FTIR spectrum at relatively low frequencies. The lower-  
18 energy absorption peaks (below  $400\text{ cm}^{-1}$ ) are mainly attributed to the vibrational modes of Ca and  
19 O atoms at the cage wall [16].  
20  
21  
22  
23

24 The symmetry of the vibrational modes at  $224$ ,  $779$  and  $848\text{ cm}^{-1}$  along with the main origin of IR  
25 bands at  $465$  and  $982\text{ cm}^{-1}$  are not assuredly determined. The absorption peaks at  $779$  and  
26  $848\text{ cm}^{-1}$  belong to the fully symmetrical mode of  $A_1$ [17]. However, the appearance of this peak in  
27 the FTIR spectrum of the film shows that  $F_2$  symmetry might also exist for these types of vibrations.  
28 In general, the high-intensity Raman absorption peaks at  $\sim 520$  and  $780\text{ cm}^{-1}$  and high-intensity FTIR  
29 peaks at  $\sim 465$  and  $848\text{ cm}^{-1}$  [18] are the most characteristic features of C12A7 vibrational behaviour .  
30  
31  
32  
33  
34  
35

36 The X-ray photoelectron spectra of the dried gel and the crystallized film are shown in  
37 Figures 4. The results were obtained for the samples before and after heat treatment in order  
38 to determine the phases present in the dried gel and the final material. A comparison between  
39 the results obtained from this experiment and the binding energies reported in the literature is  
40 presented in Table 2. The results of the analysis show that aluminium hydroxide ( $\text{Al}(\text{OH})_3$ )  
41 is formed in the dried film before the annealing treatment is carried out. The presence of  
42 aluminium hydroxide is expected as the product of aluminium sec-butoxide hydrolysis. The  
43 peak at  $289.46\text{ eV}$  (shown in the inset of figure 6) belongs to the  $\text{O-C=O}$  bond of ethyl  
44 acetate ( $\text{MeCOOEt}$ ), which is possibly formed as a result of aluminium sec-butoxide  
45 chelation with ethyl acetoacetate and remains bonded to aluminium after exposure to air. The  
46 XPS spectrum of the thin film after annealing treatment corresponds to the binding energies  
47 of C12A7 compound. The peak related to  $\text{O-C=O}$  bond has completely disappeared (inset of  
48 Figure 4(b)) which shows the decomposition of the chelating agent during the heat treatment.  
49 No separate peak was observed for the extra-framework oxygen site probably due to the  
50 binding energies of the  $\text{O}^{2-}$   $1s$  level being too close to that of the lattice and/or the  
51  
52  
53  
54  
55  
56  
57  
58  
59  
60  
61  
62  
63  
64  
65

1  
2  
3  
4 concentration of these species being too small compared to the ones of the framework  
5 oxygen ions [19].  
6

#### 7 8 **4. CONCLUSIONS** 9

10 The phase analysis of the sol-gel derived calcium aluminate thin films based on FTIR and Raman  
11 spectroscopy proved that the formation of this phase on magnesium oxide substrate is restrained at a  
12 heat treatment temperature of 1100 °C under normal air atmosphere and other calcium aluminate  
13 phases, such as C5A3, are preferably formed. An increase in the heat treatment temperature to 1300  
14 °C, however, results in the formation of single-phase C12A7 film. The heat treatment duration, on  
15 the other hand, is found to have little effect on the preferable formation of this phase over other  
16 calcium aluminate phases. It is worth mentioning that the type of extra-framework species  
17 occupying the cages in the C12A7 framework can have a significant effect on the peak positions.  
18 The vibrational behaviour of the atoms at the cage wall is affected by the presence of the species  
19 occupying the cage, the extent of which depends on the radius, mass and charge of the occupying  
20 species as well as the nature and the crystallographic position of the vibrating atom at the cage wall.  
21  
22  
23  
24  
25  
26  
27  
28  
29  
30  
31  
32

#### 33 **ACKNOWLEDGEMENTS** 34

35 The one of the authors (EF) thank Queen Mary, University of London and the LP Displays,  
36 Blackburn, UK for the PhD studentship with their financial support.  
37  
38  
39

#### 40 **References** 41

- 42 1. M. Zahedi, A. K. Ray, D. Barratt. *Sci. Adv. Mater.* 2009, **1**, 107-120.
- 43 2. S. W. Kim, Y. Toda, K. Hayashi, M. Hirano, H. Hosono, *Chem. Mater.*, 2006, **18**, 1938-1944
- 44 3. S. Matsuishi, Y. Toda, M. Miyakawa, K. Hayashi, T. Kamiya, M. Hirano, I. Tanaka, H.  
45 Hosono, *Science*, 2003, **301**, 626-629
- 46 4. P. V. Sushko, A. L. Shluger, K. Hayashi, M. Hirano, H. Hosono, *Phys. Rev. B*, 2006, **73**,  
47 014101
- 48 5. L. Palacios, A. G. De La Torre, S. Bruque, J. L. Garcia-Munoz, S. Garcia-Granda, D.  
49 Sheptyakov, M. A. G. Aranda, *Inorg. Chem.*, 2007, **46**, 4167-4176
- 50 6. Q. Chen, K. Yoshida, H. Yamamoto, M. Uchida, M. Sadakata, *Energy Fuels*, 2007, **21**, 3264–  
51 3269  
52  
53  
54  
55  
56  
57  
58  
59  
60  
61  
62  
63  
64  
65



- 1
- 2
- 3
- 4 7. M. Miyakawa, *J. Ceram. Soc. Jpn.*, 2009, **117**[3], 395-401
- 5
- 6 8. M. Miyakawaa, M. Hirano, T. Kamiya, H. Hosono, *Appl. Phys. Lett.*, 2007, **90**, 182105
- 7
- 8 9. N. Sakamoto, Y. Matsuyama, M. Hori, N. Wakiya, H. Suzuki, *Mater. Sci. Eng. B*, 2010, **173**,
- 9 21–24
- 10
- 11 10. M. Zahedi, A. K. Ray, *J Sol-Gel Sci Technol*, 2010, **55**, 317–321
- 12
- 13 11. M. Zahedi, A. K. Ray, D. S. Barratt, *J. Phys. D: Appl. Phys.*, 2008, **41**, 035404
- 14
- 15 12. Sh. Yang, J. N. Kondo, K. Hayashi, M. Hirano, K. Domen, H. Hosono, *Chem. Mater.*, 2004,
- 16 **16**, 104-110.
- 17
- 18 13. A. G. Kokhman, G. I. Zhmoidin, *Zhurnal Prikladnoi Spektroskopii* (Engl. Transl.), 1981, **35**
- 19 **[6]**, 998-1003
- 20
- 21 14. Q. Mei, C. J. Benmore, J. Siewenie, J. K. R. Weber, M. Wilding, *J. Phys.: Condens. Matter*,
- 22 2008, **20**, 245106
- 23
- 24 15. G. I. Zhmoidin, A. K. Chatterdzhi, I. I. Plyusnina, *Zhurnal Prikladnoi Spektroskopii* (Engl.
- 25 Transl.), 1972, **16** **[6]**, 1061-1066
- 26
- 27 16. A. S. Tolkacheva, S. N. Shkerin, S. V. Plaksin, E. G. Vovkotrub, K. M. Bulanin, V. A.
- 28 Kochedykov, D. P. Ordinartsev, O. I. Gyrdasova, N. G. Molchanova, *Russ. J. Appl. Chem.*,
- 29 2011, **84** **[6]**, 907-911
- 30
- 31 17. K. Kajihara, S. Matsuishi, K. Hayashi, M. Hirano, H. Hosono, *J. Phys. Chem. C*, 2007, **111**,
- 32 14855-14861
- 33
- 34 18. T. Dong, Zh. Wang, T. Kan, Q. Li, *Chin. J. Chem. Phys.*, 2007, **20** **[3]**, 297-304
- 35
- 36 19. J. A. McLeod, A. Buling, E. Z. Kurmaev, P. V. Sushko, M. Neumann, L. D.
- 37 Finkelstein, S. W. Kim, H. Hosono, A. Moewes, *Phys. Rev. B: Condens. Matter*, 2012,
- 38 **85**, 045204
- 39
- 40 20. J. T. Klopogge, L. V. Duong, B. J. Wood, R. L. Frost, *J. Colloid Interface Sci.*, 2006, **296**,
- 41 572–576
- 42
- 43 21. B. Demri, D. Muster, *J. Mater. Process. Technol.*, 1995, **55**, 311-314
- 44
- 45 22. B. V. Crist, *XPS Inter. LLC*, 2005, **2**, 59-65
- 46
- 47 23. S. Ardizzone, C.L. Bianchi, M. Fadoni, B. Vercelli, *Appl. Surf. Sci.*, 1997, **119**, 253-259
- 48
- 49
- 50
- 51
- 52
- 53
- 54
- 55
- 56
- 57
- 58
- 59
- 60
- 61
- 62
- 63
- 64
- 65

1  
2  
3  
4  
5  
6  
7  
8  
9  
10  
11  
12  
13  
14  
15  
16  
17  
18  
19  
20  
21  
22  
23  
24  
25  
26  
27  
28  
29  
30  
31  
32  
33  
34  
35  
36  
37  
38  
39  
40  
41  
42  
43  
44  
45  
46  
47  
48  
49  
50  
51  
52  
53  
54  
55  
56  
57  
58  
59  
60  
61  
62  
63  
64  
65

24. P.M. Chavhan, A. Sharma, R.K. Sharma, G. Singh, N.K. Kaushik, *Thin Solid Films*, 2010, **519** [1], 18-23

25. J. S. Corneille, J. W. He, D. W. Goodman, *Surf. Sci.*, 1994, **306** [3], 269-278

1  
2  
3  
4  
5  
6  
7  
8  
9  
10  
11  
12  
13  
14  
15  
16  
17  
18  
19  
20  
21  
22  
23  
24  
25  
26  
27  
28  
29  
30  
31  
32  
33  
34  
35  
36  
37  
38  
39  
40  
41  
42  
43  
44  
45  
46  
47  
48  
49  
50  
51  
52  
53  
54  
55  
56  
57  
58  
59  
60  
61  
62  
63  
64  
65

**Table 1** FTIR peak positions for C12A7 thin films. The related symmetry and origin of the peaks [16] are also included.

**Table 2** Raman peak positions for spin coated calcia-alumina thin films on MgO substrates which were annealed at 1300<sup>0</sup>C in air

**Table 3** Binding energy peaks and the phases formed in the film before and after heat treatment

1  
2  
3  
4 **Figure captions**  
5  
6

7 Figure 1 Microstructure of the thin film after a heat treatment at 1300 °C for 2 hr in air atmosphere  
8

9  
10 Figure 2 ATR-FTIR spectrum of the thin film annealed under air atmosphere at (a) 1300 °C for 2 hr  
11 and (b) 1100 °C for 4 hr .  
12  
13

14  
15 Figure 3 Raman spectrum of the thin film after a heat treatment under air atmosphere at (a) 1100 °C  
16 for 4 hr and (b) 1300 °C for 2 hr. The structure mainly consists of C5A3.  
17  
18

19 Figure 4: X-ray photoelectron spectrum of the thin film (a) before heat treatment (the inset  
20 shows the high resolution scan of the Carbon 1s peak) and (b) after a heat  
21 treatment at 1300 °C for 2 hr in air atmosphere ( the inset shows the high resolution  
22 scan of the Carbon 1s peak. The peak belonging to O-C=O has disappeared due to  
23 the decomposition of the chelating agent during the heat treatment.)  
24  
25  
26  
27  
28  
29  
30  
31  
32  
33  
34  
35  
36  
37  
38  
39  
40  
41  
42  
43  
44  
45  
46  
47  
48  
49  
50  
51  
52  
53  
54  
55  
56  
57  
58  
59  
60  
61  
62  
63  
64  
65

1  
2  
3  
4  
5  
6  
7  
8  
9  
10  
11  
12  
13  
14  
15  
16  
17  
18  
19  
20  
21  
22  
23  
24  
25  
26  
27  
28  
29  
30  
31  
32  
33  
34  
35  
36  
37  
38  
39  
40  
41  
42  
43  
44  
45  
46  
47  
48  
49  
50  
51  
52  
53  
54  
55  
56  
57  
58  
59  
60  
61  
62  
63  
64  
65

1  
2  
3  
4  
5  
6  
7  
8  
9  
10  
11  
12  
13  
14  
15  
16  
17  
18  
19  
20  
21  
22  
23  
24  
25  
26  
27  
28  
29  
30  
31  
32  
33  
34  
35  
36  
37  
38  
39  
40  
41  
42  
43  
44  
45  
46  
47  
48  
49  
50  
51  
52  
53  
54  
55  
56  
57  
58  
59  
60  
61  
62  
63  
64  
65

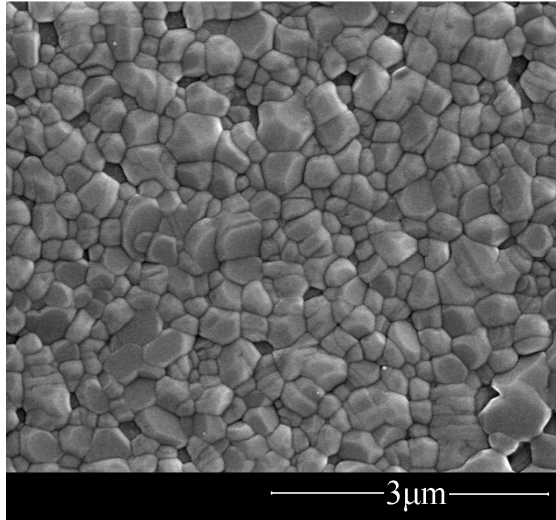
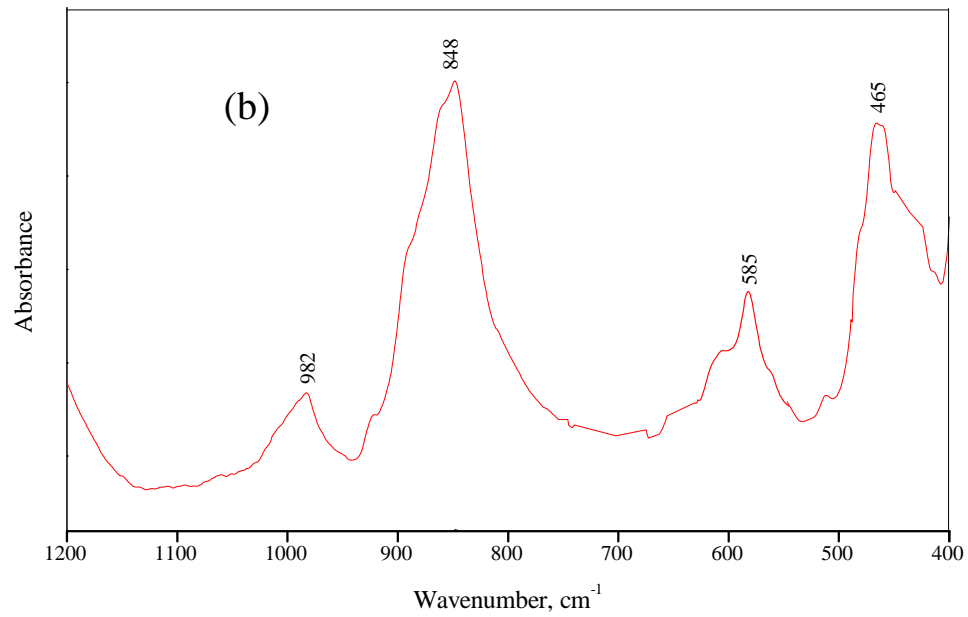
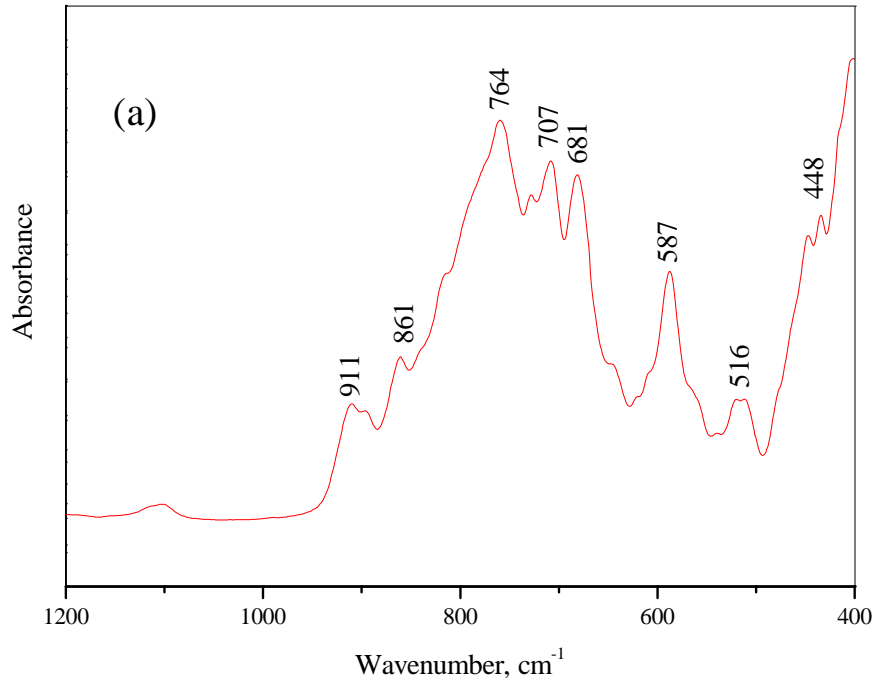


Figure 1: Microstructure of the thin film after a heat treatment at 1300 °C for 2 hr in air atmosphere



52  
53  
54  
55  
56  
57  
58  
59  
60  
61  
62  
63  
64  
65

Figure 2 ATR-FTIR spectrum of the thin film annealed under air atmosphere at (a) 1100 °C for 4 hr and (b) 1300 °C for 2 hr.

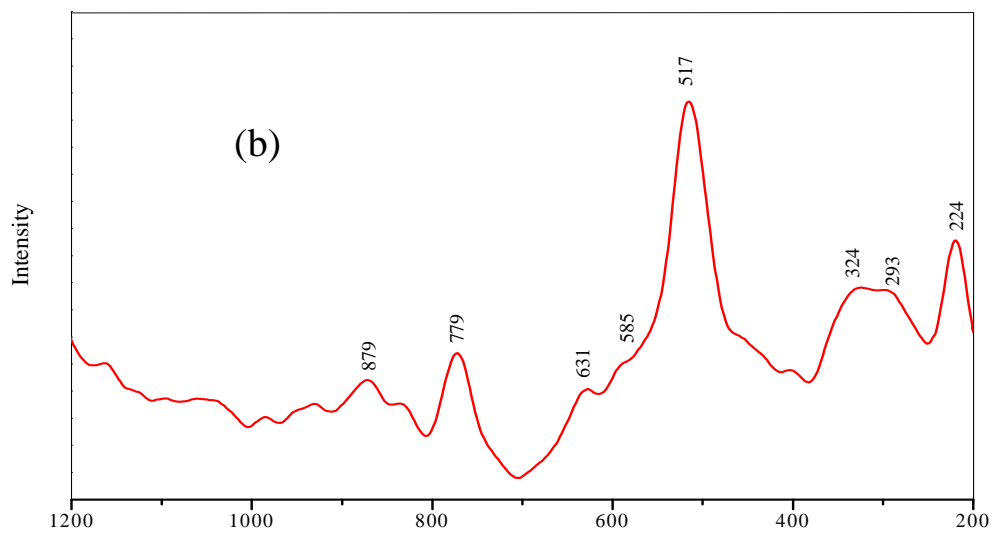
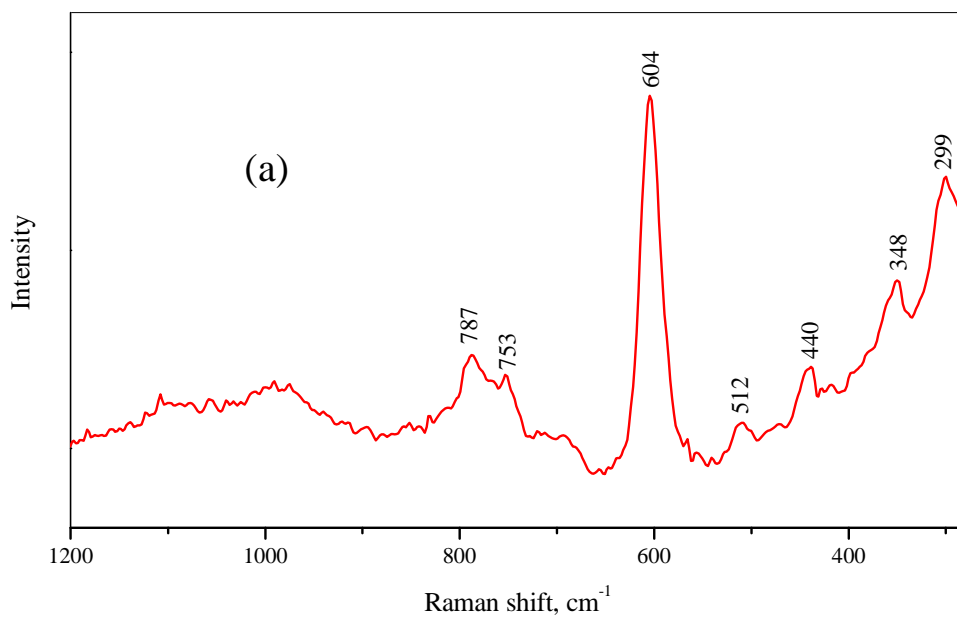


Figure 3 Raman spectrum of the thin film after a heat treatment under air atmosphere at (a) 1100 °C for 4 hr and (b) 1300 °C for 2 hr. The structure mainly consists of C5A3.



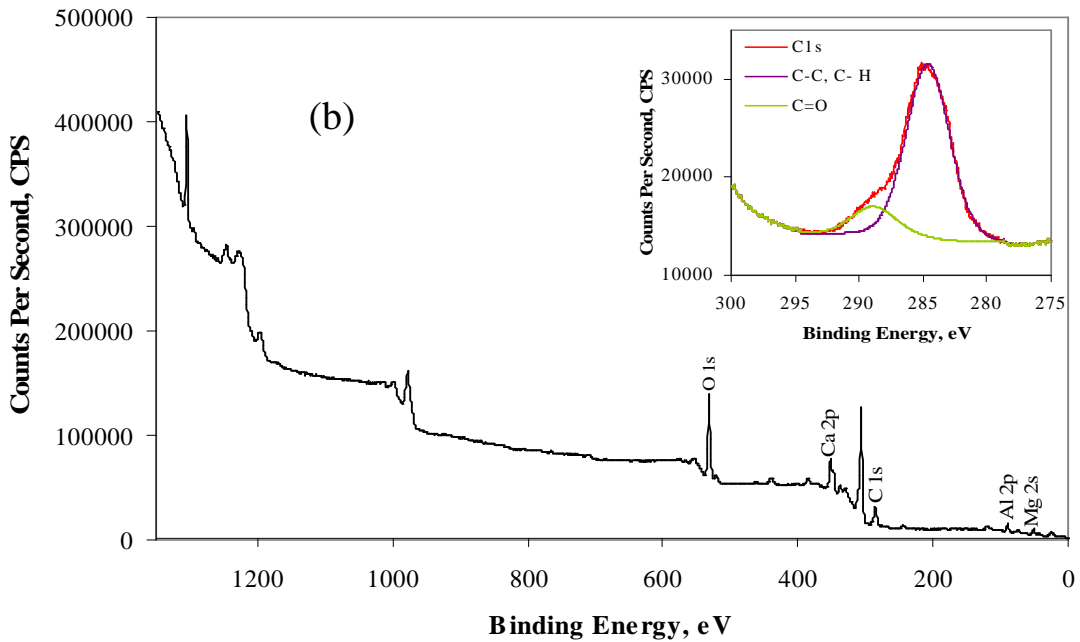
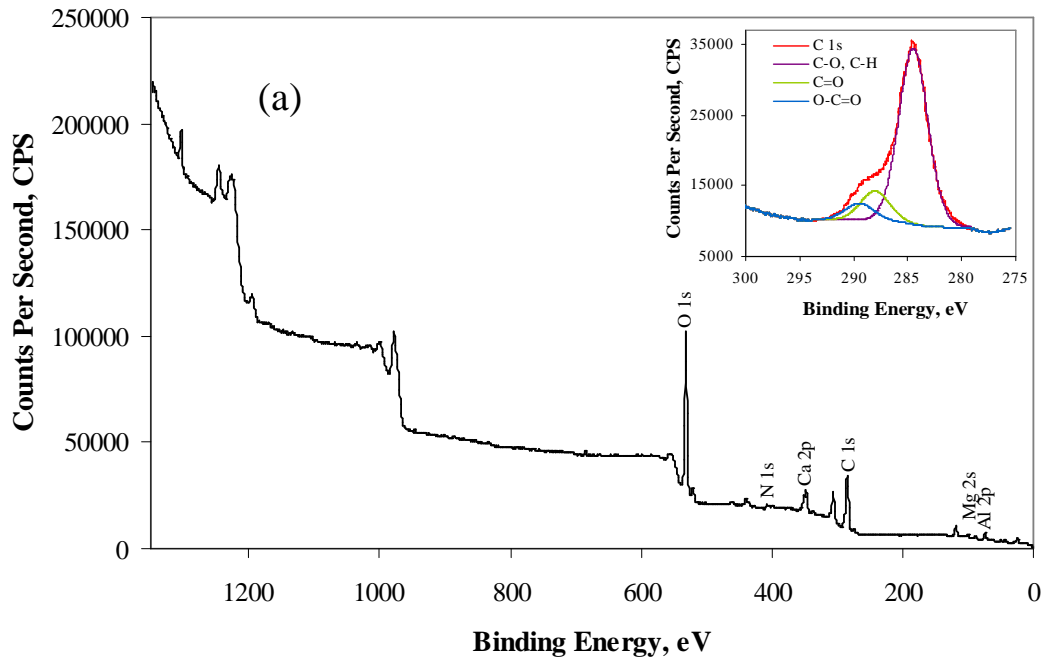


Figure 4: X-ray photoelectron spectrum of the thin film (a) before heat treatment (the inset shows the high resolution scan of the Carbon 1s peak) and (b) after a heat treatment at 1300 °C for 2 hr in air atmosphere ( the inset shows the high resolution scan of the Carbon 1s peak. The peak belonging to O-C=O has disappeared due to the decomposition of the chelating agent during the heat treatment.)

1  
2  
3  
4  
5  
6  
7  
8  
9  
10  
11  
12  
13  
14  
15  
16  
17  
18  
19  
20  
21  
22  
23  
24  
25  
26  
27  
28  
29  
30  
31  
32  
33  
34  
35  
36  
37  
38  
39  
40  
41  
42  
43  
44  
45  
46  
47  
48  
49  
50  
51  
52  
53  
54  
55  
56  
57  
58  
59  
60  
61  
62  
63  
64  
65

Table 1: FTIR peak positions for spin coated calcia-alumina thin films on MgO substrates which were annealed at 1300<sup>0</sup>Cin air

Absorption band position (cm <sup>-1</sup> )	Symmetry	Origin
465	F <sub>2</sub>	?
585	F <sub>2</sub>	Framework Al and O
848	(A <sub>1</sub> +F <sub>2</sub> ?)	Framework Al and O
982	F <sub>2</sub>	?

Table 2 Raman peak positions for spin coated calcia-alumina thin films on MgO substrates which were annealed at 1300<sup>0</sup>Cin air

Absorption band position (cm <sup>-1</sup> )	Symmetry	Origin
224	A <sub>1</sub> (+E)	Framework Ca
312	A <sub>1</sub> +F <sub>2</sub>	Framework O
326	E	Framework O
517	A <sub>1</sub>	Framework Al and O
585	F <sub>2</sub>	Framework Al and O
631		Extra-framework O
779	A <sub>1</sub> (+F <sub>2</sub> ?)	Framework Al and O
848	(A <sub>1</sub> +F <sub>2</sub> ?)	Framework Al and O
879	A <sub>1</sub>	Framework O

Table 3 Binding energy peaks and the phases formed in the film before and after heat treatment

<i>Sample treatment</i>	<i>Element</i>	<i>XPS peaks</i>		<i>Phase</i>
		<i>Experiment</i>	<i>Reference</i>	
<i>Before annealing</i>	Al 2p	73.5	73.9 [20]	Al(OH) <sub>3</sub>
	Ca 2p	347.5	348.2 [21]	Ca(NO <sub>3</sub> ) <sub>2</sub>
	N 1s	407.5	407.4 [21]	
	C 1s	289.46	289.2 [22]	MeCOOEt
	Mg 2p	50.4	50.2 [23]	MgO
<i>After annealing</i>	Al 2p	74.381	74.5 [24]	12CaO.7Al <sub>2</sub> O <sub>3</sub>
	Ca 2p	347.0	347.2 [24]	
	O 1s	531.4	531.5 [24]	
	Mg 2p	50.7	50.5-50.8 [25]	MgO